Available online at www.sciencedirect.com
SCIENCE DIRECT®

Inorganica Chimica Acta 359 (2006) 570–576

Inorganica Chimica Acta

www.elsevier.com/locate/ica

# Influence of $CH_3$ group of μ-N–C–S ligand on the properties of $[Fe_2(C_4H_5N_2S)_2(NO)_4]$ complex

N.A. Sanina, T.N. Rudneva, S.M. Aldoshin *, G.V. Shilov, D.V. Kortchagin, Yu.M. Shul'ga, V.M. Martynenko, N.S. Ovanesyan

*Institute of Problems of Chemical Physics, 1, Acad. Semenov av., 142432 Chernogolovka, Moscow Region, Russia*

Received 1 July 2005; received in revised form 6 October 2005; accepted 6 October 2005
Available online 23 November 2005

**Abstract**

Bi-nuclear neutral sulfur–nitrosyl iron complex $[Fe_2(SR)_2(NO)_4]$ (**I**) has been obtained by replacement of thiosulfate ligands in dianion $[Fe_2(S_2O_3)_2(NO)_4]^{2-}$ by 1-methyl-imidazole-2-yl. From X-ray analysis data, the complex has centrosymmetrical dimeric structure, with the iron atoms being linked via μ-N–C–S bridge. From Mossbauer spectroscopy, isomeric shift $\delta_{Fe}$ is 0.180(1) mm/s and quadrupole splitting $\Delta E_Q$ is 0.928(2) mm/s at $T = 290$ K. By comparative studying the mass-spectra in the gaseous phase of solid samples decomposition and kinetics of NO release in 1% aqueous solutions of dimethylsulfoxide, using of the ligand with $CH_3$ substituent in position 1 of imidazole-2-thiol was shown to yield a more stable donor of nitrogen monoxide than earlier obtained analog with imidazole-2-thiol, $[Fe_2(C_3H_3N_2S)_2(NO)_4]$.

*Keywords:* NO donors; Sulfur–nitrosyl iron complexes; 1-Methyl-imidazole-2-yl; X-ray analysis; Mossbauer spectroscopy; Kinetics of NO release

## 1. Introduction

Recently, intensive search has been performed for metal-based antitumor medicines of new generation with improved activity and reduced side effects as compared to available clinical medications (cisplatin, sodium nitroprusside) for therapy of oncology diseases [1–13]. The results of the latest investigations [14–21] show that medicines with antitumor activity should be sought among nitrogen monoxide donors. For example, nitrogen monoxide was shown to affect apoptosis of tumor cells, activity of gene p53, neoplasm of vessels supplying a tumor [22,23]. Binuclear paramagnetic sulfur–nitrosyl iron complexes with ligands of μ-N–C–S type ($[Fe_2(SR)_2(NO)_4]$ [24]) are synthetic analogs of natural NO donors – dinitrosyl iron complexes (DNIC), which can be detected in solutions by EPR method from a typical signal with $g = 2.03$ [25]. We suggest that different anti-neoplastic agents, i.e., structural analogs of natural aromatic thiols, in particular, mercaptohistidines used for tumor chemotherapy [26] be employed as SR ligands in $[Fe_2(SR)_2(NO)_4]$ complexes.

In this work, binuclear sulfur–nitrosyl iron complex $[Fe_2(SC_4H_5N_2)_2(NO)_4]$ (**I**) has been synthesized. 1-$CH_3$-imidazole-2-yl related to a class of pharmacologically active bidentate N,S-ligands [27] was used as a ligand for synthesis of the new NO donor of "$g = 2.03$ family". The structure and kinetics of decomposition of **I** were studied in the solid phase and solutions by X-ray analysis, IR-, Mossbauer and mass-spectroscopy, and were compared with those of earlier synthesized isostructural complex with 1-*H*-imidazole-2-yl, $[Fe_2(C_3H_3N_2S)_2(NO)_4]$ (**II**) [28].

## 2. Experimental

### 2.1. Synthesis of *I*

For synthesis, the following chemicals were used: $Na_2S_2O_3 \cdot 5H_2O$ (Aldrich), NaOH (Aldrich), 1-methyl-2-

---

* Corresponding author. Tel.: +7 095 7857048; fax: +7 096 5249676.
*E-mail addresses:* ruta@icp.ac.ru (T.N. Rudneva), sma@icp.ac.ru (S.M. Aldoshin).

0020-1693/$ - see front matter © 2005 Elsevier B.V. All rights reserved.
doi:10.1016/j.ica.2005.10.005

mercaptoimidazole (Aldrich). Complex $Na_2[Fe_2(\mu_2\text{-}S_2O_3)_2(NO)_4]\cdot4H_2O$ was synthesized according to technique [29]. The solutions preparation and mixing and the complex isolation were performed in an atmosphere of nitrogen. Solvents $CH_2Cl_2$ (Aldrich), dimethyl ether and ethanol were distilled using technique [30].

An alkali solution of thiol (21 ml, 10 mmol) was added to an aqueous solution of $Na_2[Fe_2(\mu_2\text{-}S_2O_3)_2(NO)_4]\cdot2H_2O$ (2 mmol) and $Na_2S_2O_3\cdot5H_2O$ (4 mmol) (15 ml). Immediately deposited dark-brown precipitate was filtered and washed with absolute dimethyl ether. Recrystallization from $C_2H_5OH{:}CH_2Cl_2$ (1:7) mixture yielded single crystals of (**I**) as black shining thin needle-shaped plates (Yield: 63.50%) (*Anal.* Calc. for $Fe_2S_2N_8C_8H_{10}O_4$: Fe, 24.45; S, 13.97; N, 24.45; C, 20.96; O, 13.97; H, 2.18. Found: Fe, 24.15; S, 13.79; N, 24.33; C, 21.01; H, 1.48%). IR-spectra were recorded on SPECTRUM BX-II Fourier spectrometer. The samples were used as pellets with KBr (1 mg of the substance per 300 mg of KBr): $\nu_{max}/cm^{-1}$, 3469 (m), 3149 (m), 3127 (m), 2926 (m), 2854 (m), 2362 (m), 2342 (m), 1782 (vs.), 1748 (s), 1716 (vs), 1636 (m), 1578 (m), 1534 (m), 1456 (s), 1410 (m), 1399 (m), 1367 (m), 1315 (m), 1282 (m), 1145 (s), 1087 (m), 1032 (m), 958 (m), 741 (s), 694 (s), 620 (m), 590 (m), 532 (m); 1782, 1748, 1716 (NO).

Complex **II** was synthesized using the procedure in [28].

### 2.2. X-ray analysis

Experimental data (765 reflexes with $I > 2\sigma(I)$) were obtained from the black rhomb-shaped single crystal of poor quality with the maximum linear size 0.2 mm on the automatic four-circle diffractometer KM-4 (KUMA DIFFRACTION, Poland) using monochromatic Mo Kα irradiation ($\lambda = 0.71073$ Å). An array of structural amplitudes was collected by $\omega/2\theta$-scanning in the angle range $2.59° < \theta < 26.12°$. Parameters of the unit cell were obtained and refined over 25 reflections. The crystalline structure was solved by the direct method and refined by the full-matrix least-square method in the anisotropic approximation (for the non-hydrogen atoms) using SHELX 97 Program [31]. Positions of the hydrogen atoms were calculated geometrically, their coordinates and thermal parameters were not refined. Main crystallographic data and experimental parameters are presented in Table 1. Atomic coordinates and their equivalent isotropic thermal parameters are shown in Table 2. In Table 3, inter-atomic distances and valence angles are shown.

### 2.3. Mossbauer spectroscopy

Mossbauer absorption spectra were recorded on WissEl in the mode of permanent acceleration. $Co^{57}$ in Rh matrix was used as a source. The spectra at low temperatures were measured using a flow-through helium cryostat CF-506 (Oxford Instruments) with controlled temperature. Mossbauer spectra were processed by the least-square method assuming a lorentz form for individual spectral components.

Table 1
Crystal structural data and experimental parameters for complex **I**

| Parameter | **I** |
|---|---|
| Composition | $Fe_2S_2C_8H_{10}N_8O_4$ |
| $M$ (g/mol) | 458.06 |
| $T$ (K) | 200 |
| Space group | $C2/c$ |
| $a$ (Å) | 14.455(3) |
| $b$ (Å) | 9.848(2) |
| $c$ (Å) | 13.108(3) |
| $\beta$ (°) | 116.36(3) |
| $V$ (Å$^3$) | 1671.9(6) |
| $Z$ | 4 |
| $D_{calc}$ (g/cm$^3$) | 1.820 |
| μ (mm$^{-1}$) | 2.017 |
| $2\theta_{max}$ | 56.12 |
| $N[I > 2\sigma(I)]$ | 765 |
| $N_{total}$ | 1813 |
| Goodness-of-fit | 0.864 |
| $R_1$, $wR_2$ | 0.0408, 0.0884 |

Table 2
Coordinates of the non-hydrogen atoms ($10^4\times$) and equivalent thermal parameters ($10^3\times$) in **I** (200 K)

| Atom | $X$ | $Y$ | $z$ | $U_{equiv}$ (Å$^2$) |
|---|---|---|---|---|
| Fe(1) | 3330(1) | 798(1) | 611(1) | 29(1) |
| S(1) | 1608(1) | 553(1) | −554(1) | 32(1) |
| O(1) | 3942(4) | −1858(5) | 1435(5) | 73(2) |
| O(2) | 4245(4) | 1344(5) | −851(4) | 60(1) |
| N(1) | 3655(4) | −759(6) | 1219(4) | 42(1) |
| N(2) | 3859(4) | 1236(4) | −242(4) | 33(1) |
| N(3) | 1426(3) | 2826(4) | −1840(3) | 30(1) |
| N(4) | 1218(3) | 902(5) | −2768(3) | 28(1) |
| C(1) | 1401(4) | 1479(5) | −1757(4) | 25(1) |
| C(2) | 1091(5) | 1928(6) | −3522(5) | 36(1) |
| C(3) | 1216(4) | 3114(6) | −2963(5) | 32(1) |
| C(4) | 1135(5) | −562(7) | −3010(4) | 39(1) |

### 2.4. Mass-spectroscopy

Mass-spectra of the gases released by the sample under study were recorded using mass-spectrometer MI 1201 V. The gas in the spectrometer ionic source was ionized by the electron beam of 70 eV. To obtain the gaseous phase, an 80-mg sample was placed in a quartz ampoule of the pyrolysis reactor connected to the ionization chamber through a fine control valve. The quartz ampoule with the sample was pumped out to the pressure of about $2\times10^{-5}$ Pa during an hour to remove surface and weakly bound admixtures. After pumping out, the ampoule was detached from the vacuum system and left at room temperature (≈20 °C) for about a day. Then the fine control valve was opened, and mass-spectrometric analysis of the gas in the ampoule was performed. Then the fine control valve was closed, the sample was heated to 70 °C and kept at this temperature during 1 h. The gathered gas was analyzed at this temperature. Then the quartz ampoule was again

Table 3
Inter-atomic distances and valence angles in **I** (200 K)

| *Bond length* | *d* (Å) |
|---|---|
| Fe(1)–N(1) | 1.696(5) |
| Fe(1)–N(2) | 1.667(5) |
| Fe(1)–N(3)#1 | 2.013(4) |
| Fe(1)–S(1) | 2.283(2) |
| S(1)–C(1) | 1.729(5) |
| N(1)–O(1) | 1.149(6) |
| N(2)–O(2) | 1.164(6) |
| N(3)–C(1) | 1.333(7) |
| N(3)–C(3) | 1.394(6) |
| N(3)–Fe(1)#1 | 2.013(4) |
| N(4)–C(1) | 1.356(6) |
| N(4)–C(2) | 1.367(7) |
| N(4)–C(4) | 1.470(8) |
| C(2)–C(3) | 1.347(8) |

| *Bond angle* | *Ω* (°) |
|---|---|
| N(1)–Fe(1)–N(2) | 115.8(2) |
| N(1)–Fe(1)–N(3)#1 | 108.6(2) |
| N(2)–Fe(1)–N(3)#1 | 113.2(2) |
| N(1)–Fe(1)–S(1) | 102.2(2) |
| N(2)–Fe(1)–S(1) | 105.5(2) |
| N(3)#1–Fe(1)–S(1) | 111.0(1) |
| C(1)–S(1)–Fe(1) | 104.5(2) |
| O(1)–N(1)–Fe(1) | 164.3(5) |
| O(2)–N(2)–Fe(1) | 170.2(4) |
| C(1)–N(3)–C(3) | 106.7(5) |
| C(1)–N(3)–Fe(1)#1 | 127.3(4) |
| C(3)–N(3)–Fe(1)#1 | 126.3(4) |
| C(1)–N(4)–C(2) | 107.6(4) |
| C(1)–N(4)–C(4) | 125.7(4) |
| C(2)–N(4)–C(4) | 126.6(4) |
| N(3)–C(1)–N(4) | 109.7(5) |
| N(3)–C(1)–S(1) | 126.9(4) |
| N(4)–C(1)–S(1) | 123.4(4) |
| C(3)–C(2)–N(4) | 107.8(4) |
| C(2)–C(3)–N(3) | 108.1(5) |

Operations of symmetry used for generation of equivalent atoms: #1 $-x + 1/2, -y + 1/2, -z$.

pumped out to a high vacuum, the valve was closed and the sample was heated to the next temperature (120 °C). The measurements were performed in the range $1 \leqslant m/z \leqslant 120$, $m$ – atomic weight, $z$ – the ion charge.

### 2.5. Electrochemical determination of NO

To measure concentration of NO produced by sulfur–nitrosyl iron complexes **I** and **II**, sensor electrode "amiNO-700" of "inNO Nitric Oxide Measuring System" (Innovative Instruments, Inc., Tampa, FL, USA) was used. NO concentrations were recorded during ~1 h (with 0.2-s pace) in 1% aqueous solution of DMSO with NO donor concentration 0.1 μM. DMSO was purified using method [30]. For calibration of the electrochemical sensor, a standard aqueous solution of $NaNO_2$ (100 μM) was used, which was added to the mixture of 0.12 M of KI (Aldrich) and 2 ml of 1 M $H_2SO_4$ (chemical grade) in 18 ml of water. All experiments were performed in aerobic solutions at 25 °C. pH of the solutions were measured using a membrane pH-meter HI 8314 (HANNA Instruments, Germany). Processing of experimental spectra and calculation of decomposition constants for complexes **I** and **II** have been performed using program complex *Origin 6.1*.

## 3. Results and discussion

### 3.1. Scheme of [Fe$_2$(SC$_4$H$_5$N$_2$)$_2$(NO)$_4$] synthesis

Complex (**I**) was obtained by replacement of thiosulfate ligands by 1-methyl-imidazole-2-yl according to

$$S[Fe_2(S_2O_3)_2(NO)_4]^{2-} + 2S_2O_3^{2-} \rightarrow 2[Fe(S_2O_3)_2(NO)_2]^{3-} \xrightarrow[-4S_2O_3^{2-}]{+2C_4H_5N_2S^-, OH^-} [Fe_2(SC_4H_5N_2)_2(NO)_4] \qquad (1)$$

**I** is well soluble in DNSO, DMFA, acetone, THF, acetonitrile and *o*-xylene, partially soluble in methanol, dimethyl ether and carbon tetrachloride, poorly soluble in ethanol. In acetonitrile, acetone, methylene chloride, *o*-xylol, $CCl_4$ and THF it decomposes in a few minutes after dissolving to yield a beige (in acetonitrile) or dirty-green (*o*-xylene) amorphous precipitate or brown suspension. **I** is insoluble in *n*-heptane and isopropyl alcohol.

### 3.2. Structure of [Fe$_2$(SC$_4$H$_5$N$_2$)$_2$(NO)$_4$] complex

By incorporating substituents, physical–chemical properties of nitrosyl products, such as solubility, stability in the solid phase and solutions, coordination opportunities of a ligand, can be varied [32], this being important for application of such systems in biologic and medical studies.

Sulfur–nitrosyl iron complex **I** forms according to scheme (1), and it contains the ligand differing from that involved in complex **II** by the presence of –$CH_3$ group in position 1 of 2-mercaptoimidazole. As follows from the analysis of IR-spectrum of complex **I**, there is no absorption band $\nu$(N–H) at 3495 cm$^{-1}$, this being typical for **II**, and two bands $\delta^a(CH_3)$ at 1456 cm$^{-1}$ and $\delta^s(CH_3)$ at 1368 cm$^{-1}$ can be observed. A low-intensity absorption band $\delta^s(CH_3)$ is nonmonotonic background and might be shifted to lower wave numbers. It is more difficult to identify stretching vibrations of $CH_3$ group because of the presence of many low-intensity absorption bands in the region of 2950–2800 cm$^{-1}$.

From X-ray data, **I** has a centrosymmetric dimeric binuclear structure (Fig. 1), similar to that of earlier studied binuclear sulfur–nitrosyl complex **II** with imidazole-2-yl [28]. In the dimer, two tetrahedral-coordinated iron atoms are linked by Fe–S–C–N–Fe′ bridge. The methyl-imidazole ligand is bidentate and is able to coordinate according to a thiol (Fig. 2(a)) and thion (Fig. 2(b)) type. A little shortened bond lengths in the structure of **I**, N(3)–C(1) 1.333(7) Å, C(2)–C(3) 1.347(8) Å, as compared to the other bonds in the cycle, N(4)–C(1) 1.356(6) Å, N(3)–C(3) 1.394(6) Å, N(4)–C(2) 1.367(7) Å and S(1)–C(1) 1.729(5) Å, and the bond length C(1)–S(1) 1.729(5) Å

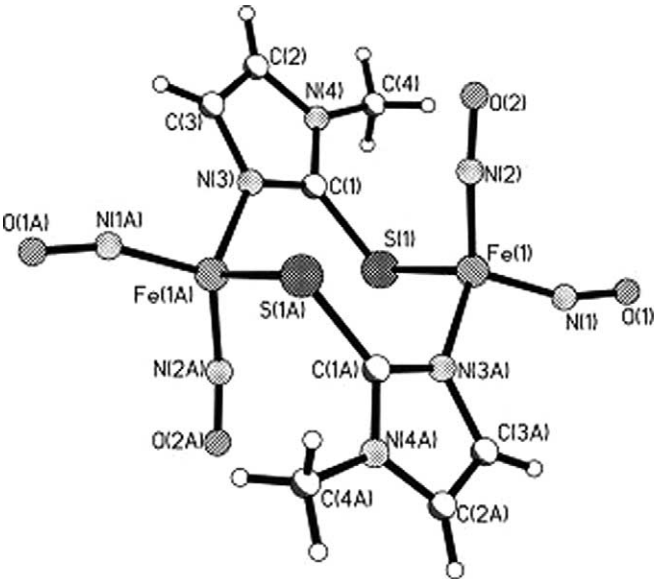

Fig. 1. Structure of $[Fe_2(\mu\text{-}SC_4H_5N_2)_2(NO)_4]$ and atoms numeration.

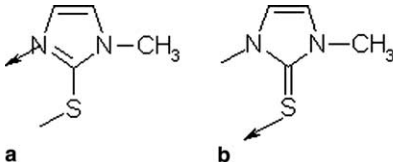

Fig. 2. Prototropic tautomery and dissociation of 1-methyl-2-mercaptoimidazole.

exceeding the length of the double S=C bond (1.684 Å), suggest that the ligand is present in the complex in the thiol form (Fig. 2(a)). The bond lengths Fe(1)–S(1) and Fe(1)–N(3) are 2.283(2) Å and 2.013(4)(7) Å, respectively.

Mossbauer spectrum of **I** looks like a single doublet thus suggesting equivalence of iron atoms, this being consistent with X-ray data. It should be also noted that in **I** bond Fe–S is a little shorter than that in **II** (2.299(1) Å). From Mossbauer spectroscopy data, in **I** the value of isomeric shift ($\delta = 0.180(1)$ mm/s) is less than in isostructural **II** ($\delta = 0.196(1)$ mm/s). The decrease of isomeric shift value points to the increase of s-electron density on the iron atom (we have noted this in [33]) and, accordingly, to the reduction of Fe–S bond length in **I**. The Fe–Fe distance in **I** is shorter (4.02 Å) than in **II** (4.10 Å).

Three planes can be marked out in the molecular structure of **I**: S(1)C(1)N(4)C(2)C(3)N(3)Fe(1A) {1}, S(1)Fe(1)S(1A)Fe(1A) {2}, S(1A)C(1A)N(4A)C(2A)C(3A)N(3A)Fe(1) {3}. The molecule has a "chair" shape, with planes {1} and {2}, {2} and {3} intersecting at 68.1°. The values of these dihedral angles are somewhat less than those in **II** (70.6° [28]). Lability of the bond lengths distribution in the Fe–N–O fragment was found out in other complexes, too [34]. It is assumed [35] that in the $Fe(NO)_2$ fragment even internal disproportionation is possible to the point of complete oxidation–reduction to yield $(ON)^+$–Fe–$(NO)^-$. A partial oxidation–reduction in Fe–NO fragment is possible because of easy direct $d_{Fe} \rightarrow \pi^*_{NO}$ and reverse donation, which is accompanied by shortening/elongation of Fe–N and elongation/shortening of N–O bonds with simultaneous change of the Fe–N–O group valence. Structural lability of the Fe–N–O fragment also appears in the difference of stretching N–O vibrations in IR-spectra [36]. The difference between the frequencies of two absorption bands in **I** ($\Delta\nu_{NO}$) is 68 $cm^{-1}$, whereas this value in the spectrum of complex **II** is 55 $cm^{-1}$. The increase of $\Delta\nu_{NO}$ value suggests that NO groups in **I** are less equivalent than those in **II**, this being confirmed by X-ray data for complex **I**.

In structural fragment $Fe(NO)_2$, bond lengths N(1)–O(1) 1.149(6) Å and N(2)–O(2) 1.164(6) Å, Fe(1)–N(1) 1.696(5) Å and Fe(1)–N(2) 1.667(5) Å differ, though they are similar to those in **II**, and angles O(1)–N(1)–Fe(1) (163.4(5)°) and O(2)–N(2)–Fe(1) (170.2(4)°) also differ (by 6.8°).

The crystalline structure of the studied complex (Fig. 3) consists of the layers parallel to plane bc and linked by weak H···O and H···S contacts. Each corrugated layer is

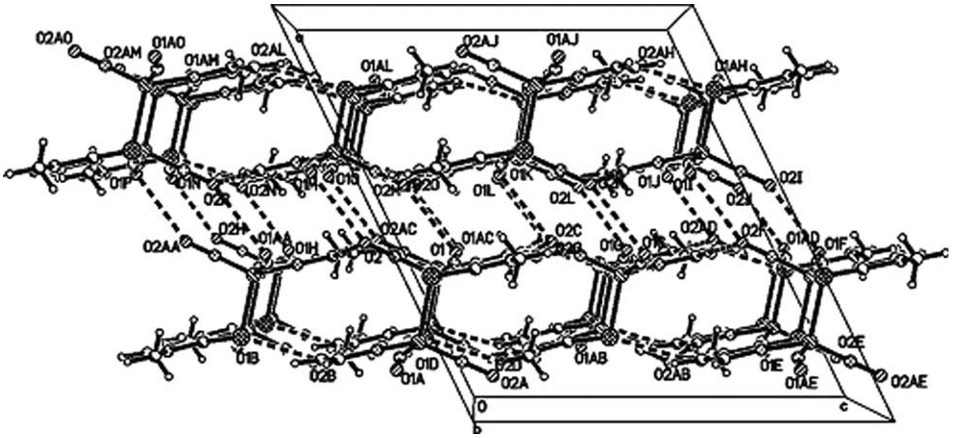

Fig. 3. The fragment of the crystalline structure of **I** (projection on *ac* plane).

displaced with regard to another by 1/2 of the translation along axis *c*. Inter-molecular contacts of two types were detected between molecules of the same layer: (1) C(3)–H(2)···O(2)′ 2.593 Å, ∠C(3)–H···O(2)′ 178.0°; (2) C(4)–H(5)···S(1)′ 2.815 Å, ∠C(4)–H···S(1)′ 149.3°. Molecules of different layers are directed to each other by NO groups, with a distance between them being O(1)···O(2)′ 3.09 Å. Apparently, the layers are linked by electrostatic forces.

In solutions, as was found out earlier [37], activation of the NO groups of sulfur–nitrosyl complex involves the initial stage of the Fe–S bond rupture and formation of a mononuclear dinitrosyl complex. It can be assumed that replacement of H by $CH_3$ group in the ligand, which was used for the present synthesis, results in the formation of sulfur–nitrosyl iron complex **I**, which is more stable than complex **II** (this being evidenced by shortening of the Fe–S bond and intra-molecular Fe···Fe distance). This assumption is confirmed by the properties of the complex in the solid phase and in solutions.

### *3.3. Mass-spectrum investigation of complexes **I** and **II***

Figs. 4 and 5 show mass-spectra of **I** and **II** under heating. Both complexes are quite stable in vacuum at room temperature. Pressure of the gases gathered while keeping the samples in vacuum did not practically exceed the level of residual gases in the mass-spectrometer. While heating from 20 to 70 °C, **I** appeared to be more stable than **II**. The main component of the gas released by **I** is NO (the ion with $m/z = 30$). In addition to the peak due to NO molecules, peaks with $m/z = 14$ ($[N]^+$), 18 ($[H_2O]^+$), 28 ($[CO]^+$ and/or $[N_2]^+$) and 44 ($[CS]^+$ and/or $[CO_2]^+$) can be seen in the mass-spectrum. Arising of $[N]^+$ and $[H_2O]^+$ ions is obvious (nitrogen is present in the nitrosyl group, and water is adsorbed by crystals). Molecules CO, $CO_2$ and $N_2$ may be captured during the sample contacts with air.

The captured and, hence, weakly bound molecules should have been released into the gaseous phase upon pumping. But they did not show in the spectra of gases

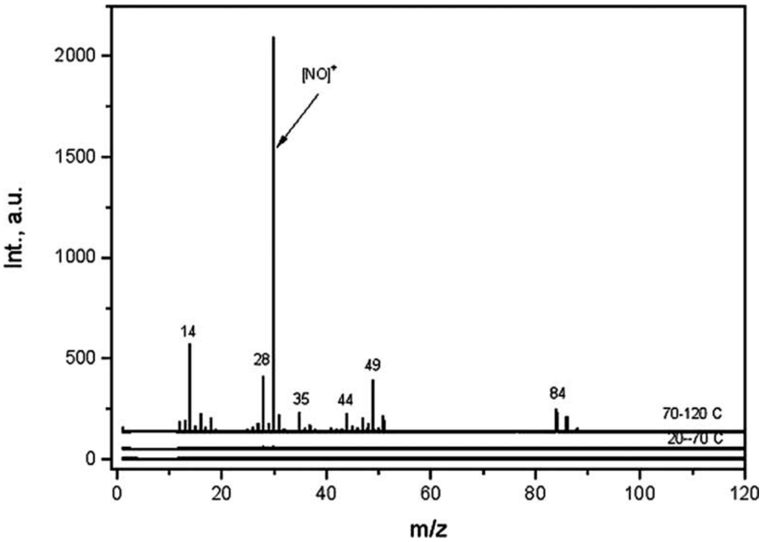

Fig. 4. Mass-spectrum of gases generated by **I** under heating.

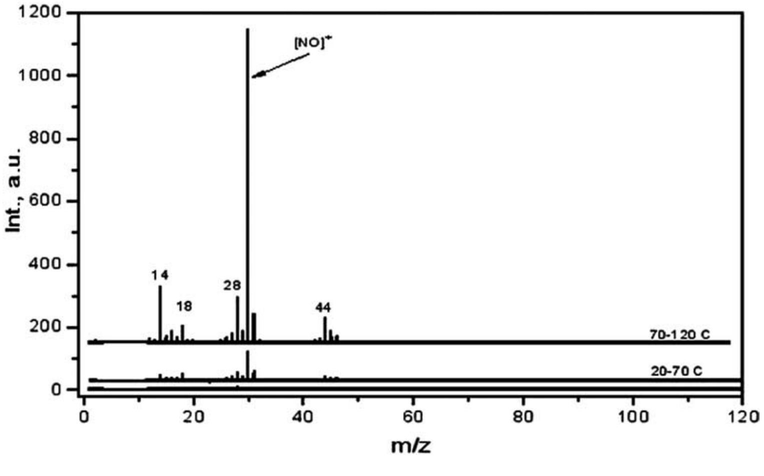

Fig. 5. Mass-spectrum of gases generated by **II** under heating.

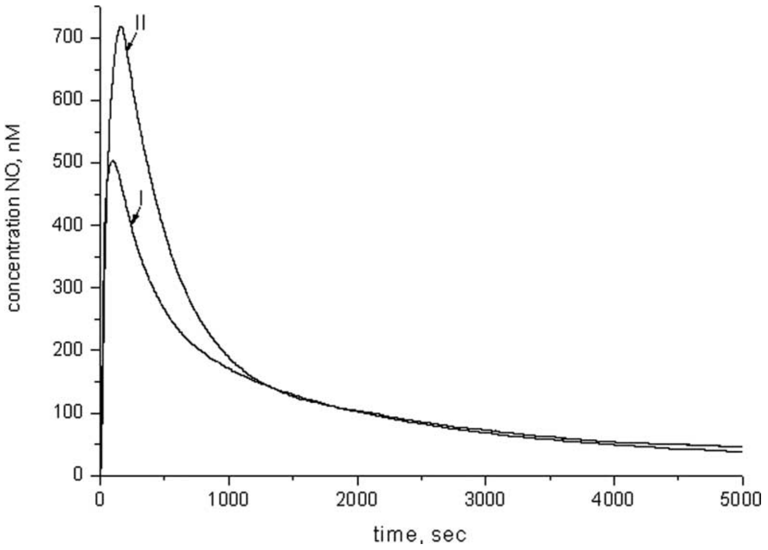

Fig. 6. Dependence of varying the concentration of NO generated upon decomposition of sulfur–nitrosyl iron complexes **I** and **II** ($1 \times 10^{-4}$ M/l) in 1% DMSO water solutions at 25 °C vs. time.

obtained after the sample was kept in vacuum without heating. The assumption can be made that peaks with $m/z = 24$ and 44 are due to $[N_2]^+$ and $[CS]^+$ fragments of imidazole $C_3H_3N_2S$, respectively. The presence of the peaks with $m/z = 45$ ($[HCS]^+$) and 46 ($[H_2CS]^+$) in the spectra is another confirmation of the assumption about a possible transfer of the ligand or products of its decomposition into the gaseous phase. However, no other ligand fragments were detected in the spectrum of this sample.

Thus, heating to 70 °C does not result in noticeable gasification of sample **I**, while **II** releases NO and $H_2O$ molecules into the gaseous phase upon such heating. Heating from 70° to 120° intensifies gasification of both samples. For **II**, the composition of the gaseous phase did not change, but the pressure of the released gas increased essentially. For sample **I** the spectrum of the gaseous phase in this temperature range had the largest number of peaks. In addition to NO and $H_2O$ molecules, there is a noticeable amount of ligand molecules $C_4H_5N_2S$ and the products of its decomposition in the gaseous phase.

### 3.4. Kinetics of NO release by complexes *I* and *II*

Fig. 6 and Table 4 present the data on kinetics of NO release by complexes **I** and **II**. Kinetic curves in Fig. 6 describe the release of NO and its reactions with $O_2$, which is available in the solutions. The release and consumption of NO in proton medium start during a sample preparation. In aerobic experiments, using a sensor electrode, we register not the initial concentration of NO generated by NO-donors, but the amount of NO consumed in its reaction with oxygen in time. We assume that decomposition of complexes **I** and **II** occurs according to scheme:

$$A \xrightarrow{k_1} P \xrightarrow{k_2} B$$

where A is a complex; P is NO generated by the complex; B is the products of NO and $O_2$ interaction.

$O_2$ concentration in the solution is $1.36 \times 10^{-3}$ mol/l [38], and this is higher than concentration of NO generated by complexes **I** and **II** in the performed experiments ($6.4 \times 10^{-7}$ mol/l). Therefore, we assume that decomposition of complexes **I** and **II** is the first order reaction. The rate constants of the complexes decomposition are shown in Table 4, and they are consistent with the statement that complex **I** is more stable in solutions than complex **II**.

Dependence of NO release by complexes **I** and **II** on time in anaerobic solutions under similar conditions will be studied in our further research.

Table 4
Rate constants for decomposition of complexes **I** and **II** in aerobic water solutions ($T = 25°$)

| NO-donor | $pH_{ini}/pH_{final}$ | $k_1$ ($s^{-1}$) | $k_2$ ($s^{-1}$) |
|---|---|---|---|
| $[Fe_2(SC_4H_5N_2)_2(NO)_4]$ (**I**) | 5.50/5.77 | $1.10 \times 10^{-3}$ | $343.2 \times 10^{-3}$ |
| $[Fe_2(C_3H_3N_2S)_2(NO)_4]$ (**II**) | 5.55/5.57 | $1.72 \times 10^{-3}$ | $373.2 \times 10^{-3}$ |

## 4. Conclusion

It has been shown by the investigations performed that using of aza-heterocyclic ligand, namely, the derivative of imidazole-2-thiol with substituent $CH_3$ in position 1 of the imidazole cycle, results in the formation pf binuclear sulfur–nitrosyl iron complex of μ-N–C–S type, which is a more stable donor of nitrogen monoxide in the solid phase and in solutions than earlier obtained analog $[Fe_2(C_3H_3N_2S)_2(NO)_4]$.

## 5. Supplementary materials

Crystallographic data have been deposited with the Cambridge Crystallographic Data Centre, CCDC No. 273835. Copies of the data can be obtained free of charge on application to CCDC, The Director, 12 Union Road, Cambridge CB2 2EZ, UK (fax: +44 1223 336033; e-mail: deposit@ccdc.cam.ac.uk or http://www.ccdc.cam.ac.uk).

## Acknowledgements

The work has been performed with the financial support of the Russian Foundation for Basic Research (Grant No. 04-03-08108) and the Program of the Russian Academy of Sciences "Fundamental problems of medicine"

## References

[1] D. Chatterjee, A. Mitra, A. Sengupta, S. Basak, Inorg. Chim. Acta 358 (2005) 22.
[2] R. Meyer, S. Brink, C.E.J. van Rensburg, G.K. Joone, H. Görls, S. Lotz, J. Organometall. Chem. 690 (2005) 117.
[3] M. Markovic, N. Kneževic, S. Momčilovic, S. Grguric-Sipka, L. Harhaji, V. Trajkovic, M.M. Stojkovic, T. Sabo, D. Miljkovic, Eur. J. Pharmacol. 517 (2005) 28.
[4] Sh. Nafiti, A. Sobhanmanesh, M. Esm-Hosseini, K. Alimoghaddam, H.A. Tajmir-Riahi, J. Mol. Struct. 750 (2005) 22.
[5] Q. Li, H.F.C. Guedes da Silva, Zh. Jinghua, A.J.L. Pombeiro, J. Organometall. Chem. 689 (2004) 4581.
[6] F. Liang, P. Wang, X. Zhou, T. Li, Z. Li, H. Lin, D. Gao, C. Zheng, C. Wu, Bioorg. Med. Chem. Lett. 14 (2004) 1901.
[7] Z.-D. Xu, H. Liu, S.-L. Xiao, M. Yang, X.-H. Bu, J. Inorg. Biochem. 90 (2000) 79.
[8] J. Bariyanga, A.S. Luyt, J. Mol. Struct. 559 (2001) 49.
[9] E. Melendez, M. Marrero, C. Rivera, E. Harnandez, A. Segal, Inorg. Chim. Acta 298 (2000) 178.
[10] V.M. Gonzalez, M.A. Fuertes, M.J. Perez-Alvarez, G. Cervantes, V. Moreno, C. Alonso, J.M. Perez, Biochem. Pharmacol. 60 (2000) 371.
[11] G. Cervantes, S. Marchal, M.J. Prieto, J.M. Perez, V.M. Gonzalez, C. Alonso, V. Moreno, J. Inorg. Biochem. 77 (1999) 197.
[12] S. Marchal, V. Moreno, G. Aullon, S. Alvarez, M. Quiros, M. Font-Bardia, X. Solans, Polyhedron 18 (1999) 3675.
[13] D. Kong, C. Qin, L. Meng, Y. Xie, Bioorg. Med. Chem. Lett. 9 (1999) 1087.
[14] O. Siri, A. Tabard, P. Pullumbi, R. Guilard, Inorg. Chim. Acta 350 (2003) 633.
[15] J.L. Burgaud, E. Jngini, Del Soldato P. Ann, N.Y. Acad. Sci. 962 (2002) 360.
[16] T.I. Karu, L.V. Pyatibrat, G.S. Kalendo, Toxicol. Lett. 121 (2001) 57.
[17] A.F. Vanin, Vestnik Rossiiskoi Akademii Nauk 4 (2000) 3.
[18] Kh. Maeda, T. Akauke, Biochemistry 63 (1998) 7, 1007.
[19] P.K. Lala, Cancer Metastas. Rev. 17 (1998) 1.
[20] J. Oszajca, G. Stochel, E. Wasielewska, Z. Stasicka, R.J. Gryglewski, A. Jakubowski, K. Cieslik, J. Inorg. Biochem. 69 (1998) 121.
[21] D. Wink, J. Vodovoz, J. Cook, Biochemistry 63 (1998) 7, 948.
[22] U.K Messmer, M. Ankarerona, P. Nicotera, B. Brune, FEBS Lett. 21 (1994) 335, 1, 23.
[23] B. Brune, N. Scheneiderhan, Toxicol. Lett. 193 (2003) 2, 19.
[24] N.A. Sanina, S.M. Aldoshin, Russ. Chem. Bull., Int. Ed. 53 (2004) 11, 2428.
[25] A.R. Butler, I.L. Megson, Chem. Rev. 102 (2002) 1155.
[26] J. Jolley, W.I. Gross, R.G. Pritchard, Ch.A. McAuliffe, K.B. Nolan, Inorg. Chim. Acta 315 (2001) 36.
[27] A. Silvestri, G. Ruisi, M.A. Girasolo, J. Inorg. Biochem. 92 (2002) 171.
[28] N.A. Sanina, S.M. Aldoshin, T.N. Rudneva, N.I. Golovina, G.V. Shilov, Yu.M. Shulga, N.S. Ovanesyan, V.N. Ikorskiy, V.I. Ovcharenko, J. Mol. Struct. 752 (2005) 110.
[29] O.A. Rakova, N.A. Sanina, Yu.M. Shulga, V.M. Martynenko, N.S. Ovanesyan, S.M. Aldoshin, Doklady Chem. 383 (2002) 1, 75.
[30] A. Weissberger, E. Proskauer, J.A. Riddick, E.E. Toops, Organic Solvents: Physical Properties and Methods of Purification, 1955.
[31] G.M. Sheldrick, SHELX-97, Release 97-2, Program for Crystal Structure Refinement, University of Göttingen, Germany, 1997.
[32] P.D. Akrivos, Coord. Chem. Rev. 213 (2001) 181.
[33] N.A. Sanina, S.A. Aldoshin, Izv. Akad. Nauk, Ser. Khim. 11 (2004) 2326.
[34] S.M. Aldoshin, N.A. Sanina, O.A. Rakova, G.V. Shilov, A.V. Kulikov, Yu.I. Shul'ga, N.S. Ovanesyan, Russ. Chem. Bull., Int. Ed. 52 (2003) 8, 1702.
[35] A.F. Vanin, B. Muller, J.L. Alencar, I.I. Lobysheva, F. Nepveu, J.-C. Stoclet, Nitric Oxide: Biology and Chemistry 7 (2002) 194.
[36] M. Fontecave, J.-L. Pierre, Bull. Soc. Chem. Fr. 131 (1994) 620.
[37] S.V. Vasilieva, E.Yu. Moshkovskaya, N.A. Sanina, T.N. Rudneva, A.V. Kulikov, S.M. Aldoshin, Dokl. Biol. 402 (2005) 230.
[38] B.V. Nekrasov (Ed.), Desk Chemical Reference book, Moscow, 1955, p. 261.